Exploration of a Metabolism-Related Gene Signature Predicting Prognosis for Ovarian Cancer

Jinling Zhang (dr_jlzhang@163.com)
Shenzhen People's Hospital https://orcid.org/0000-0002-6017-7751
Yifan Zhang
Shenzhen People's Hospital
Lin Zhang
Shenzhen People's Hospital
Haili Li
Shenzhen People's Hospital

Research Article

Keywords: Ovarian cancer, Metabolism-related genes, Signature, Prognosis, Immune microenvironment

Posted Date: September 23rd, 2021

DOI: https://doi.org/10.21203/rs.3.rs-917465/v1

Abstract

Background: Dysregulation of metabolism plays a critical role in the pathogenesis and progression of ovarian cancer (OC). However, the expression pattern of metabolic genes in OC and the prognostic value of metabolism-related genes for OC patients remains to be elucidated. Thus, this study aimed to identify a metabolism-related prognostic gene signature for OC.

Methods: The expression profiles of metabolism-related genes and associated clinicopathological characteristics were obtained from online datasets (The Cancer Genome Atlas, TCGA and The Genotype-Tissue Expression, GTEx). The differently expressed genes were subjected to functional enrichment analysis. By means of LASSO, univariate and multivariate Cox regression analyses, this predictive signature was constructed and validated by internal and external databases. Genomic alterations, immune infiltration, tumor microenvironment, and drug sensitivity associated with the signature were also described.

Results: A total of 302 metabolism-related differentially expressed genes were identified. These genes were mainly enriched in functions associated with substance and energy metabolism. Based on the 302 identified genes, a prognostic signature of 21 metabolic genes was constructed and validated across internal and external cohorts. The patients in the high-risk group had significantly longer overall survival compared to those in the low-risk group. By univariate and multivariate Cox regression, the signature was identified as an independent prognostic predictor for overall survival. There were also noticeable differences with regards to genetic alteration, immune infiltration, tumor microenvironment and drug sensitivity between the two groups.

Conclusion: Our study suggests that clinical outcomes of OC patients are associated with dysregulated metabolic genes and that the metabolism-related prognostic signature can be used as a predictor for the overall survival of OC patients.

Introduction

Ovarian cancer (OC) is one of the most common cancers arising in the female reproductive system. Although novel diagnostic methods and advanced therapies have been adopted to delay recurrence and death, the overall prognosis remains poor. The estimated 5-year relative survival rate of OC patients is only 48.6%[1]. As the leading cause of death in women with gynecological cancers, OC is responsible for 14,000 deaths in the United States in 2020[2], seriously threatening women's lives and health[3].

Accurate assessment of mortality risk and identification of high-risk patients are key to prognosis improvement. Risk stratification makes it possible to deliver timely and appropriate interventions. However, an effective indicator to predict the prognosis of OC is still lacking. In the past decades, researchers have paid much attention to the roles of oncogenes and tumor suppressor genes in the pathogenesis of OC. But the association between these genes and overall survival is still ambiguous[4, 5]. Some studies showed a better prognosis for patients with BRCA1/BRCA2 germline mutations, while others suggested that BRCA1/BRCA2 mutation is not an independent prognostic factor for long-term survival[6, 7]. It has also been proposed that the presence of circulating tumor cells (CTCs) prior to the treatment is associated with poorer overall survival (OS) and progression-free survival (PFS) in patients with OC[8]. But since the capture of CTCs is expensive and technically demanding, its clinical application is rather limited. Therefore, an effective prediction model is still needed for accurate assessment of patient prognosis.

In the past decade, the understanding of tumor cell metabolism has greatly improved. Metabolic reprogramming is considered an emerging hallmark of malignancy. The essence of neoplasm involves not only uncontrolled cell growth and division, but also dysregulation of metabolism, which provides energy and substances for cell proliferation, migration and invasion[9, 10]. In the early 1920s, Otto Warburg found that cancer cells largely limit energy metabolism to glycolysis, even under aerobic conditions. This phenomenon is known as the "Warbury effect"[11]. In addition to aerobic glycolysis, mitochondrial oxidative phosphorylation, glutamine metabolism, the reverse Warburg effect, and the truncated tricarboxylic acid cycle are also critical in metabolic reprogramming of cancer cells[12, 13]. Recent studies further highlight the metabolic heterogeneity between tumors and even within different regions of solid tumors, where cancer cells can participate in a variety of metabolic programs to meet growth and proliferation requirements[14]. Metabolic processes have been shown to play an important role in the pathogenesis and progression of OC. Abnormalities in phospholipid metabolism, L-tryptophan metabolism, fatty acid beta-oxidation, and piperidine derivatives were found in OC[15]. As shown by metabolomic profiling, the levels of tryptophan, alanine, and methionine in tumor tissues were significantly reduced, while the levels of 3-hydroxybutyric acid and 3,4-dihydroxybutyric acid were significantly increased in OC patients compared to patients with benign lesions. This may be explained by the up-regulation of fatty acid oxidation metabolic pathways in OC tissues[16]. Another metabolomic analysis showed enhanced mitochondrial function in cisplatin-resistant ovarian cancer cells compared to cisplatin-sensitive cells, associated with enzymatic changes of the electron transport chain and mitochondrial coupling [17]. Further studies revealed that dysregulated levels of serum metabolites are associated with patient prognosis. Metabolic profiling and novel biomarkers of serum have been applied in the prediction of overall survival (OS) and discrimination of short-term mortality for OC patients [18]. Nevertheless, the expression pattern of metabolism-related genes mediating metabolic reprogramming in OC tissues has not been thoroughly investigated.

Therefore, we aim to explore the aberrant expression of metabolic genes in tumor tissues and their correlations with the overall survival of OC patients. In this study, we identified differentially expressed metabolic genes and established a metabolism-related gene signature predicting prognosis for OC based on bioinformatics and statistical analysis of data from The Cancer Genome Atlas (TCGA) database and the Genotype-Tissue Expression (GTEx) database. The model was further validated in an external cohort from the Gene Expression Omnibus (GEO) database. Tumor mutation status and immune microenvironment in the high-risk score phenotype of the signature was also compared to those of the low-risk phenotype. In conclusion, our results revealed that dysregulated metabolic genes are associated with clinical outcomes of OC patients, and provides an effective model for prognosis prediction and risk stratification, which could potentially be used in clinical scenarios.

Materials & Methods

Data Acquisition and Preprocessing

The expression profile and clinical information of OC in TCGA (https://xena.ucsc.edu/) were downloaded, and 378 samples with complete clinical information were selected. Expression profiles of all normal tissue samples were obtained from GTEx (https://www.gtexportal.org/), and expression profiles of 180 normal ovarian tissues were extracted. The dataset GSE63885 (n = 101 cases) [19] was downloaded from GEO (https://www.ncbi.nlm.nih.gov/geo) as an independent external validation set. 75 Samples with complete clinical information were included. The clinical information of OC patients in different data sets is shown in Table 1. And mutation data of OC were obtained from TCGA. The dataset GSE63885 obtained from GEO was obtained with the GPL570 platform. The probes were mapped to genes. The highest expression was selected if multiple probes corresponded to the same gene. The batch effect between different data sets from the same platform was removed using the R package “Limma”[20]. For all analyses, gene expression levels were logarithmically transformed and normalized.

Table 1
Clinical information of patients with OV in different data sets

Characteristics	TCGA Training Set	GEO Validation Set
Number of samples	378	75
Median survival time(days)	1024	1105
Number of death (%)	232(61.38)	66(88)
Average age(years)	59.55	NA
FIGO stage (%)		
I	1(0.26)	0(0.00)
II	23(6.08)	2(2.67)
III	294(77.78)	63(84.00)
IV	57(15.08)	10(13.33)
Grade (%)		
1	1(0.26)	0(0.00)
2	45(11.90)	9(12.00)
3	321(84.92)	48(64.00)
4	1(0.26)	18(24.00)

Differential Expression Analysis

The batch effect between data from TCGA and GTEx was removed using the R package “Edge”. Differential expression analysis between the two groups was performed. False discovery rater (FDR) and fold change (FC) were calculated. Genes showing altered expression with FDR < 0.05 and |logFC|>2 was were considered as differentially expressed genes (DEGs).

GO and KEGG Functional Enrichment Analyses

70 metabolism-related gene sets were obtained from Kyoto Encyclopedia of Genes and Genomes (KEGG) pathways (https://www.gsea-msigdb.org/gsea/index.jsp). A total of 1466 genes were identified as metabolism-related. Using R package “clusterProfiler”, the gene ontology (GO) enrichment including biological processes (BP), cellular components (CC) and molecular function (MF) were conducted and KEGG analysis was performed for metabolism-related DEGs. FDR < 0.05 was considered significant.

Construction and Validation of Metabolism-Related Gene Signature for OC

378 OC samples from TCGA were used as a training set to construct the signature. Cox regression was performed for univariate analysis with the R package “survival”. P < 0.05 was considered significant. Metabolism-related DEGs that were associated with overall survival (OS) were included in LASSO regression (R package “glmnet”). Dimensionality reduction techniques were further used to screen prognostic genes. A prognosis assessment model was constructed based on LASSO regression. The genes involved in the model and the coefficients were also obtained by LASSO regression.

The risk scores of all 378 OC samples from TCGA were calculated according to the model, and the patients were divided into high- and low-risk groups according to the median score. The difference in overall survival between the two groups was assessed by a log-rank test. The model was further validated in an external cohort from the GEO database (GSE63885).

Assessment of Mutation and Microenvironment

Genetic alteration and drug sensitivity analysis of the prognostic genes in the gene signature were investigated using cBioportal (https://www.cbioportal.org/)[21] and GSCALite (http://bioinfo.life.hust.edu.cn/web/GSCALite/)[22] platforms respectively. Analyses of mutation, immune score and matrix score were performed using R packages “maftools” and “estimate”. The status of immune infiltration in OC patients was achieved by the online platform CIBERSORT (http://cibersort.stanford.edu/). Patients were divided into high- and low-risk groups according to risk scores and differences between the two groups were compared. All statistical analyses in this study were completed by R, version 3.6.1.

Results

Identification of Differentially Expressed Metabolism-Related Genes in OC patients

The expression profiles of 378 samples of OC patients from TCGA and 180 samples of normal ovarian tissues from GTEx were obtained. Removal for batch effect and differential expression analysis between the two groups were performed. FDR < 0.05 and |logFC|>2 was set as thresholds. A total of 4622 differentially expressed genes were identified, among which 1487 genes were up-regulated and 3135 were down-regulated. Heat map of top the 100 differentially expressed genes was constructed for hierarchical clustering, with |logFC| ranked from large to small (Fig. 1).

The 4622 DEGs between OC and normal ovarian tissues were intersected with 1466 metabolism-related genes identified in KEGG pathways. We obtained 302 differentially expressed genes that were involved in metabolic pathways (Fig. 2).

Functional Enrichment Analysis of Metabolism-Related DEGs

To understand the functions of metabolism-related DEGs, GO and KEGG enrichment analyses were performed for the annotation of genes. Our results revealed that the differentially expressed metabolism-related genes were significantly enriched in the biological processes associated with small molecule catabolic process, carboxylic acid biosynthetic process, organic acid biosynthetic process, glycoprotein metabolic process, glycoprotein biosynthetic process and sulfur compound metabolic process. As for cellular components, the metabolism-related DEGs were enriched in components of mitochondrial inner membrane, respiratory chain, respiratory chain complex, mitochondrial respiratory chain, and mitochondrial membrane part. According to molecular functions, these genes were typically enriched in transferase activity, oxidoreductase activity, monooxygenase activity, iron ion binding and UDP-glycosyltransferase activity. Analysis of KEGG pathway also showed that the metabolic DEGs were enriched in oxidative phosphorylation, metabolism of xenobiotics by cytochrome P450, drug metabolism, purine metabolism and chemical carcinogenesis (Fig. 3).

The Prognostic Signature of Metabolism-Related Genes

378 OC samples from TCGA were used as the training set to construct the prognostic signature. We performed univariate COX regression and identified 27 metabolism-related DEGs that were significantly associated with OS among 302 genes. As shown in Fig. 4, according to the results of Cox regression analysis, patients were divided into two groups based on the median levels of gene expression and significant difference of OS was observed between the two groups, indicating good prognostic effects of the selected genes.

The 27 metabolism-related DEGs were included in LASSO regression for further dimensionality reduction, and 21 prognostic genes were selected (Fig. 5). Based on the LASSO regression, a prognostic signature composing of 21 genes was constructed from the LASSO results (Fig. 6) (Table 2). The risk score was calculated by the formula:

$$\varvec{Risk}\varvec{Score} = \sum_{\varvec{i}=1}^{\varvec{n}} \left(\exp(\text{gene})_{\varvec{i}} * \text{coef}(\text{gene})_{\varvec{i}} \right)$$

Table 2
LASSO regression results

No.	Signature	Coef
1	ACSM1	-0.003185055
2	AGPAT4	7.82E-05
3	ALDH1L1	0.000202394
4	CSGALNACT1	0.000313545
5	CYP2S1	3.41E-05
6	DCT	0.002533373
7	DGKD	2.89E-05
8	DHRS9	0.000304884
9	GALNT10	0.000108406
10	GFPT2	0.000137715
11	LYPLA1	-2.24E-05
12	MIF	-4.40E-06
13	PDE10A	5.29E-05
14	PDE7B	0.000165216
15	PLA2G2D	-0.000684144
16	PRPS2	-2.08E-05
17	TPMT	-2.57E-05
18	UGT2B15	0.002619482
19	UQCRFS1	8.86E-06
20	UST	0.000160528
21	WARS	-2.43E-05

In the training set, the risk score of each OC patient from TCGA was calculated according to the signature using coefficients generated by LASSO regression. And all the 378 OC patients were divided into low- and high-risk groups based on the median score of the training set. The result of the log-rank test showed that the overall survival of the low-risk group was significantly longer than that of the high-risk group ($p < 0.001$). The model was further validated in GSE63885, an external cohort from the GEO database. The OS was significantly longer for patients with lower risk scores (Fig. 7).

Verification of the Model as an Independent Predictor

In addition to risk scores obtained from the metabolism-related gene signature, clinicopathological data, such as age, clinical stage, histologic grade, cancer status, tumor residual and primary diagnosis, were included in regression analyses. By applying univariate and multivariate Cox regression, the signature consisting of 21 genes was identified as an independent prognostic predictor for OS (Table 3).

Table 3
Multivariate Cox regression analysis of the prognostic signature

Variable	Univariate analysis			Multivariate analysis		
	HR	95%CI	P-Value	HR	95%CI	P-Value
RiskScore	4.65	3.44–6.27	**< 0.001**	2.81	1.96–4.03	**< 0.001**
Age	1.02	1.01–1.03	**0.001**	1.01	1-1.03	0.128
Clinical stage	1.31	0.99–1.74	0.062	-	-	-
Histologic grade	1.24	0.84–1.84	0.279	-	-	-
Cancer status	8.39	4.55–15.46	**< 0.001**	7.55	3.67–15.57	**< 0.001**
Tumor residual	1.31	1.15–1.5	**< 0.001**	1.06	0.9–1.24	0.501
Race	1.24	1.03–1.49	**0.025**	1.09	0.89–1.35	0.397
Primary diagnosis	3.71	0.92–15.03	0.066	-	-	-

Gene Alteration and Tumor Microenvironment Patterns Associated with Prognostic Signature

Genetic alteration and drug sensitivity analysis of the prognostic genes in the gene signature were investigated using cBioportal and GSCALite. As expected, amplification was the most common form of alteration in these metabolic genes (Fig. 8). As for the drug sensitivity analysis, low expression of DCT and DGKD was associated with drug resistance, while high expression of TPMT was associated with drug resistance (Fig. 9).

The samples in the training set were divided into high- and low-risk groups according to the median risk score calculated by the signature, and the mutation spectrums of two groups were shown in Fig. 10. Missense mutation was the most common form of gene alteration in both groups.

CIBERSORT algorithm was used to assess the immune cell infiltration in the high- and low-risk groups. We found that among 22 types of immune cell, T cells CD4 memory resting, T cells CD4 memory activated, T cells regulatory Tregs, monocytes, and macrophages M1 showed different infiltrating patterns between two groups. Specifically, infiltration of T cells CD4 memory resting and monocytes was more common in the high-risk group than in the low-risk group ($p = 0.00865$, $p = 0.00493$), while the infiltration of T cells CD4 memory activated, T cells regulatory Tregs and macrophages M1 were more common in the low-risk group ($p = 0.00839$, $p = 0.03828$, $p < 0.0001$), as shown in Fig. 11.

According to the results of the Estimate, both immune score and matrix score were significantly different between the high- and low-risk groups. The immune score of the high-risk group was lower than that of the low-risk group. The matrix score, however, was higher in the high-risk group (Fig. 12).

Discussion

With the rapid development of biotechnology, metabolic reprogramming is no longer limited to alterations in glycolysis and the tricarboxylic acid cycle but is further extended to fatty acid metabolism, glutamine metabolism, and serine metabolism. Some studies have shown that metabolic reprogramming not only affects the biosynthesis and energy metabolism of tumor cells but also exerts regulatory effects on the immune response process through various metabolic enzymes and metabolic molecules, ultimately influencing tumor development and progression[23, 24]. Sugar and glutamine are the main sources of energy for the rapid proliferation of ovarian cancer cells. Hyperglycemia, as a presenting feature of overweight and obesity, is associated with tumorigenesis and poor prognosis, and may increase the risk of OC[25]. In terms of glutamine metabolism, highly invasive ovarian cancer cells were significantly dependent on glutamine, and high expression of glutamine synthetase is associated with poor prognosis in OC patients[26, 27]. Thus, tumor metabolism is not only associated with the development of OC, but also affects patient prognosis. However, an effective prognostic signature for OC based on metabolism-related genes is still lacking.

In this study, a prognostic signature consisting of 21 metabolic genes was developed based on the training set from TCGA and GTEx, and validated in an independent external dataset from GEO. The results showed a poor prognosis for OC patients with higher risk scores. Moreover, the results of univariate and multivariate Cox regression indicated that this prognostic signature could be used as an independent prognostic factor for OS. As expected, the differentially expressed metabolic genes were mainly enriched in functions associated with metabolism, including oxidative phosphorylation, cytochrome P450 enzyme exogenous substance metabolism, cytochrome P450 enzyme drug metabolism, and purine metabolism, reflecting potential molecular mechanisms of dysregulated genes in the metabolic microenvironment of OC. In addition, there was a significant difference in terms of immune cell infiltration, immune score, and stromal score between the high- and low-risk groups.

Most of the 21 metabolic genes in the signature have been reported to be associated with malignancy. Previous studies have reported that up-regulated expression of Agpat4 in colorectal cancer (CRC) tissues is strongly associated with poor prognosis[28]. ALDH1L1, a candidate tumor suppressor, is often silenced in tumor tissues and is positively correlated with tumorigenesis and invasiveness[29]. The glycosylation enzymes CSGALNACT1, GALNT10 and GFPT2 were overexpressed in prostate cancer, high grade ovarian serous cancer (HGSC) and lung adenocarcinoma, respectively. They were also found to play a key role in various biological processes in tumorigenesis, including immune surveillance and cell metabolism[30–32]. CYP2S1 has been reported

to be largely associated with cell proliferation and lipid metabolism, and the downregulation of CYP2S1 was reported to promote proliferation of CRC cells[33]. Inhibition of DGKD expression reduces the proliferation of castration-resistant and androgen-dependent prostate cancer cells[34]. DHRS9 expression is reduced in oral squamous cell carcinoma tissues, and low expression of DHRS9 is strongly associated with tumor progression and poor prognosis. Significant upregulation of LYPLA1 was observed in non-small cell lung cancer (NSCLC) cells in vitro, which is found to be pro-tumorigenic[35]. PDE7B can degrade intracellular cAMP, which inhibits cell cycle arrest and apoptosis of cancer cells. At present, elevated expression of PDE7B has been detected in various malignant tumors, and it negatively impacts survival[36]. PRPS2 promotes nucleotide biosynthesis, which drives cancer initiation and progression[37]. Another study confirmed that PRPS2 is significantly up-regulated in prostate adenocarcinoma and is strongly associated with progression[38]. As for UGT2B15 and UQCRFS1, they were involved in glucuronidation and electron transfer in the mitochondrial respiratory chain, respectively. Both were found overexpressed in gastric cancer, with overexpression of UGT2B15 negatively correlated with the prognosis[39, 40]. MIF, PDE10A, PLA2G2D, and WARS are primarily involved in immunomodulation and inflammatory response[41–44].

To further uncover the biological implications of the prognostic genes in the signature, we explored gene mutation and tumor microenvironment of the two groups. Genetic alterations were found in all these prognostic metabolic genes in OC, with amplification being the most common type. Missense mutation is the most common in both the high- and low-risk groups. It has been previously reported that an increase, decrease in genomic copy number, or other mutations could result in alterations in gene expression [45]. These alterations may be the potential mechanism for dysregulated expression of 21 metabolic genes in the prognostic signature. As for the drug sensitivity analysis, the results indicated that DCT, DGKD and TPMT could be potential biomarkers for drug screening.

The results of immune cell infiltration indicated that there are a variety of immune cells that are significantly different between the high- and low-risk groups, and the immune score of the high-risk group is lower than the low-risk group. It has been confirmed that the higher metabolic activity greatly impacts the nutrient composition of the tumor microenvironment, which may have a critical impact on the local immune response[46]. There is growing evidence that the metabolism and function of T cells are restricted by dysregulated glycolysis in tumor tissues, thereby impairing the immune response[47, 48]. For example, the expression of tumor-associated glycolysis-related genes was negatively correlated with T-cell infiltration in melanoma and NSCLC patients compared to controls [49]. Recent studies have reported that, compared with healthy controls, Teff cells from cancer patients show reduced activity and dysfunction of mitochondria, thus failing to achieve substantial cell division and anti-tumor immune effects[50]. This is consistent with our findings that Tregs infiltration was less common in the high-risk group than the low-risk group. Meanwhile, pieces of evidence suggest that tumor growth is promoted by itaconic acid-mediated immunomodulation[51]. Metabolomics revealed that immune-responsive gene 1 (IRG1) modulated immune response by catalyzing the production of itaconic acid, directly linking metabolism to immunity [52]. Weiss et al verified that itaconic acid promotes fatty acid oxidation-mediated oxidative phosphorylation and glycolysis, by up-regulating macrophages in ovarian cancer tissues. In addition, the expression of IRG1 was significantly elevated in monocytes from OC patients. Consistently, our study observed different infiltration patterns of monocytes and macrophages between two groups, implying potential roles of these cells in tumorigenesis. Overall, these studies reveal that the metabolic reprogramming in cancer patients has a pivotal impact on the local and systemic immune response, which is closely related to tumor progression and patient prognosis.

Admittedly, there are still some limitations to the study. First, since additional clinical information, such as metabolic disorders and therapies, cannot be obtained from the databases, we were unable to assess the association between our model and these aspects. Second, the patients from different databases had diverse ethnic and cultural backgrounds. Thus, we should be cautious when applying the model in a certain population and more independent cohort studies are needed to validate the signature. Also, more basic research is needed to clarify the specific roles of metabolic genes in the pathogenesis and progression of OC.

Conclusions

In conclusion, we constructed a prognostic metabolic signature for OC based on the TCGA database and GTEx database, and verified the prognostic value of our signature with the GEO database. The metabolic genes involved in the model are associated with dysregulation of both metabolic and immune microenvironment. Our results provide an effective model for prognosis prediction and risk stratification, which could potentially be used in clinical practice. But still, there is a need to validate our signature in more independent cohort studies.

Declarations

Acknowledgements

The information of this study is obtained by the TCGA, GTEx, and GEO database. We are grateful for the source of data used in our study.

Author Contributions

Yifan Zhang presented the idea, performed data analysis, and prepared the manuscript. Yuting Xiang re-analyzed all the data, verified the results, and made substantial revision of the manuscript. Lin Zhang edited the manuscript. Jinling Zhang made specific design of the study and participated in manuscript preparation. Hailing Li participated in study design, data analysis and manuscript preparation. All authors read and approved the final manuscript.

Funding

The authors received no funding for this work.

Availability of Data and Materials

The public datasets used in our work can be found on https://xena.ucsc.edu/, https://www.gtexportal.org/, https://www.ncbi.nlm.nih.gov/geo.

Ethics Approval and Consent to Participate

Not applicable.

Consent for Publication

Not applicable.

Competing Interests

The authors declare that they have no competing interest.

References

1. Eisenhauer EA. Real-world evidence in the treatment of ovarian cancer. Ann Oncol. 2017;28:viii61–5.
2. Siegel RL, Miller KD, Jemal A. Cancer statistics, 2020. CA Cancer J Clin. 2020;70:7–30.
3. Hutchcraft ML, Gallion HH, Kolesar JM. **MUTYH as an Emerging Predictive Biomarker in Ovarian Cancer**. *Diagnostics (Basel)* 2021, 11.
4. Zhang M, Zhuang G, Sun X, Shen Y, Wang W, Li Q, Di W. TP53 mutation-mediated genomic instability induces the evolution of chemoresistance and recurrence in epithelial ovarian cancer. Diagn Pathol. 2017;12:16.
5. Nielsen FC, van Overeem Hansen T, Sørensen CS. Hereditary breast and ovarian cancer: new genes in confined pathways. Nat Rev Cancer. 2016;16:599–612.
6. Kotsopoulos J, Rosen B, Fan I, Moody J, McLaughlin JR, Risch H, May T, Sun P, Narod SA. Ten-year survival after epithelial ovarian cancer is not associated with BRCA mutation status. Gynecol Oncol. 2016;140:42–7.
7. Arts-de Jong M, de Bock GH, van Asperen CJ, Mourits MJ, de Hullu JA, Kets CM. Germline BRCA1/2 mutation testing is indicated in every patient with epithelial ovarian cancer: A systematic review. Eur J Cancer. 2016;61:137–45.
8. Huang C, Lin X, He J, Liu N. **Enrichment and detection method for the prognostic value of circulating tumor cells in ovarian cancer: A meta-analysis**. *Gynecol Oncol* 2021.
9. Ghesquière B, Wong BW, Kuchnio A, Carmeliet P. Metabolism of stromal and immune cells in health and disease. Nature. 2014;511:167–76.
10. Hanahan D, Weinberg RA. Hallmarks of cancer: the next generation. Cell. 2011;144:646–74.
11. Petersen MC, Vatner DF, Shulman GI. Regulation of hepatic glucose metabolism in health and disease. Nat Rev Endocrinol. 2017;13:572–87.
12. Weinberg F, Hamanaka R, Wheaton WW, Weinberg S, Joseph J, Lopez M, Kalyanaraman B, Mutlu GM, Budinger GR, Chandel NS. Mitochondrial metabolism and ROS generation are essential for Kras-mediated tumorigenicity. Proc Natl Acad Sci U S A. 2010;107:8788–93.
13. Yoshida GJ. Metabolic reprogramming: the emerging concept and associated therapeutic strategies. J Exp Clin Cancer Res. 2015;34:111.
14. Kim J, DeBerardinis RJ. Mechanisms and Implications of Metabolic Heterogeneity in Cancer. Cell Metab. 2019;30:434–46.
15. Ke C, Hou Y, Zhang H, Fan L, Ge T, Guo B, Zhang F, Yang K, Wang J, Lou G, Li K. Large-scale profiling of metabolic dysregulation in ovarian cancer. Int J Cancer. 2015;136:516–26.
16. Hilvo M, de Santiago I, Gopalacharyulu P, Schmitt WD, Budczies J, Kuhberg M, Dietel M, Aittokallio T, Markowetz F, Denkert C, et al. Accumulated Metabolites of Hydroxybutyric Acid Serve as Diagnostic and Prognostic Biomarkers of Ovarian High-Grade Serous Carcinomas. Cancer Res. 2016;76:796–804.
17. Ghoneum A, Gonzalez D, Abdulfattah AY, Said N. **Metabolic Plasticity in Ovarian Cancer Stem Cells**. *Cancers (Basel)* 2020, 12.
18. Xie H, Hou Y, Cheng J, Openkova MS, Xia B, Wang W, Li A, Yang K, Li J, Xu H, et al. Metabolic profiling and novel plasma biomarkers for predicting survival in epithelial ovarian cancer. Oncotarget. 2017;8:32134–46.
19. Lisowska KM, Olbryt M, Student S, Kujawa KA, Cortez AJ, Simek K, Dansonka-Mieszkowska A, Rzepecka IK, Tudrej P, Kupryjańczyk J. Unsupervised analysis reveals two molecular subgroups of serous ovarian cancer with distinct gene expression profiles and survival. J Cancer Res Clin Oncol. 2016;142:1239–52.
20. Diboun I, Wernisch L, Orengo CA, Koltzenburg M. Microarray analysis after RNA amplification can detect pronounced differences in gene expression using limma. BMC Genom. 2006;7:252.
21. Gao J, Aksoy BA, Dogrusoz U, Dresdner G, Gross B, Sumer SO, Sun Y, Jacobsen A, Sinha R, Larsson E, et al. Integrative analysis of complex cancer genomics and clinical profiles using the cBioPortal. Sci Signal. 2013;6:pl1.
22. Liu CJ, Hu FF, Xia MX, Han L, Zhang Q, Guo AY. GSCALite: a web server for gene set cancer analysis. Bioinformatics. 2018;34:3771–2.

23. Gomes AP, Blenis J. A nexus for cellular homeostasis: the interplay between metabolic and signal transduction pathways. Curr Opin Biotechnol. 2015;34:110–7.
24. Lue HW, Podolak J, Kolahi K, Cheng L, Rao S, Garg D, Xue CH, Rantala JK, Tyner JW, Thornburg KL, et al. Metabolic reprogramming ensures cancer cell survival despite oncogenic signaling blockade. Genes Dev. 2017;31:2067–84.
25. Nagle CM, Kolahdooz F, Ibiebele TI, Olsen CM, Lahmann PH, Green AC, Webb PM. Carbohydrate intake, glycemic load, glycemic index, and risk of ovarian cancer. Ann Oncol. 2011;22:1332–8.
26. Yang L, Moss T, Mangala LS, Marini J, Zhao H, Wahlig S, Armaiz-Pena G, Jiang D, Achreja A, Win J, et al. Metabolic shifts toward glutamine regulate tumor growth, invasion and bioenergetics in ovarian cancer. Mol Syst Biol. 2014;10:728.
27. Fan S, Wang Y, Zhang Z, Lu J, Wu Z, Shan Q, Sun C, Wu D, Li M, Sheng N, et al. High expression of glutamate-ammonia ligase is associated with unfavorable prognosis in patients with ovarian cancer. J Cell Biochem. 2018;119:6008–15.
28. Zhang D, Shi R, Xiang W, Kang X, Tang B, Li C, Gao L, Zhang X, Zhang L, Dai R, Miao H. The Agpat4/LPA axis in colorectal cancer cells regulates antitumor responses via p38/p65 signaling in macrophages. Signal Transduct Target Ther. 2020;5:24.
29. Krupenko SA, Horita DA. The Role of Single-Nucleotide Polymorphisms in the Function of Candidate Tumor Suppressor ALDH1L1. Front Genet. 2019;10:1013.
30. Munkley J, Vodak D, Livermore KE, James K, Wilson BT, Knight B, McCullagh P, McGrath J, Crundwell M, Harries LW, et al. Glycosylation is an Androgen-Regulated Process Essential for Prostate Cancer Cell Viability. EBioMedicine. 2016;8:103–16.
31. Zhang G, Lu J, Yang M, Wang Y, Liu H, Xu C. Elevated GALNT10 expression identifies immunosuppressive microenvironment and dismal prognosis of patients with high grade serous ovarian cancer. Cancer Immunol Immunother. 2020;69:175–87.
32. Zhang W, Bouchard G, Yu A, Shafiq M, Jamali M, Shrager JB, Ayers K, Bakr S, Gentles AJ, Diehn M, et al. GFPT2-Expressing Cancer-Associated Fibroblasts Mediate Metabolic Reprogramming in Human Lung Adenocarcinoma. Cancer Res. 2018;78:3445–57.
33. Yang C, Li C, Li M, Tong X, Hu X, Yang X, Yan X, He L, Wan C. CYP2S1 depletion enhances colorectal cell proliferation is associated with PGE2-mediated activation of β-catenin signaling. Exp Cell Res. 2015;331:377–86.
34. Whitworth H, Bhadel S, Ivey M, Conaway M, Spencer A, Hernan R, Holemon H, Gioeli D. Identification of kinases regulating prostate cancer cell growth using an RNAi phenotypic screen. PLoS One. 2012;7:e38950.
35. Mohammed A, Zhang C, Zhang S, Shen Q, Li J, Tang Z, Liu H. Inhibition of cell proliferation and migration in non–small cell lung cancer cells through the suppression of LYPLA1. Oncol Rep. 2019;41:973–80.
36. Zhang DD, Li Y, Xu Y, Kim J, Huang S. Phosphodiesterase 7B/microRNA-200c relationship regulates triple-negative breast cancer cell growth. Oncogene. 2019;38:1106–20.
37. Cunningham JT, Moreno MV, Lodi A, Ronen SM, Ruggero D. Protein and nucleotide biosynthesis are coupled by a single rate-limiting enzyme, PRPS2, to drive cancer. Cell. 2014;157:1088–103.
38. Qiao H, Tan X, Lv DJ, Xing RW, Shu FP, Zhong CF, Li C, Zou YG, Mao XM. Phosphoribosyl pyrophosphate synthetases 2 knockdown inhibits prostate cancer progression by suppressing cell cycle and inducing cell apoptosis. J Cancer. 2020;11:1027–37.
39. Chen X, Li D, Wang N, Yang M, Liao A, Wang S, Hu G, Zeng B, Yao Y, Liu D, et al. Bioinformatic analysis suggests that UGT2B15 activates the Hippo–YAP signaling pathway leading to the pathogenesis of gastric cancer. Oncol Rep. 2018;40:1855–62.
40. Jun KH, Kim SY, Yoon JH, Song JH, Park WS. Amplification of the UQCRFS1 Gene in Gastric Cancers. J Gastric Cancer. 2012;12:73–80.
41. Kang I, Bucala R. The immunobiology of MIF: function, genetics and prospects for precision medicine. Nat Rev Rheumatol. 2019;15:427–37.
42. Titulaer MJ, Irani SR, Lassmann H. **PDE10A antibodies in autoimmune encephalitis: A possible marker of cancer immunotherapy?** *Neurology* 2019, 93:327–328.
43. Miki Y, Kidoguchi Y, Sato M, Taketomi Y, Taya C, Muramatsu K, Gelb MH, Yamamoto K, Murakami M. Dual Roles of Group IID Phospholipase A2 in Inflammation and Cancer. J Biol Chem. 2016;291:15588–601.
44. Cheong JH, Yang HK, Kim H, Kim WH, Kim YW, Kook MC, Park YK, Kim HH, Lee HS, Lee KH, et al. Predictive test for chemotherapy response in resectable gastric cancer: a multi-cohort, retrospective analysis. Lancet Oncol. 2018;19:629–38.
45. Pollack JR, Sørlie T, Perou CM, Rees CA, Jeffrey SS, Lonning PE, Tibshirani R, Botstein D, Børresen-Dale AL, Brown PO. Microarray analysis reveals a major direct role of DNA copy number alteration in the transcriptional program of human breast tumors. Proc Natl Acad Sci U S A. 2002;99:12963–8.
46. Biswas SK. Metabolic Reprogramming of Immune Cells in Cancer Progression. Immunity. 2015;43:435–49.
47. Kishore M, Cheung KCP, Fu H, Bonacina F, Wang G, Coe D, Ward EJ, Colamatteo A, Jangani M, Baragetti A, et al. Regulatory T Cell Migration Is Dependent on Glucokinase-Mediated Glycolysis. Immunity. 2017;47:875–89.e810.
48. Chang CH, Qiu J, O'Sullivan D, Buck MD, Noguchi T, Curtis JD, Chen Q, Gindin M, Gubin MM, van der Windt GJ, et al. Metabolic Competition in the Tumor Microenvironment Is a Driver of Cancer Progression. Cell. 2015;162:1229–41.
49. Cascone T, McKenzie JA, Mbofung RM, Punt S, Wang Z, Xu C, Williams LJ, Wang Z, Bristow CA, Carugo A, et al. Increased Tumor Glycolysis Characterizes Immune Resistance to Adoptive T Cell Therapy. Cell Metab. 2018;27:977–87.e974.
50. Leone RD, Powell JD. Metabolism of immune cells in cancer. Nat Rev Cancer. 2020;20:516–31.
51. Weiss JM, Davies LC, Karwan M, Ileva L, Ozaki MK, Cheng RY, Ridnour LA, Annunziata CM, Wink DA, McVicar DW. Itaconic acid mediates crosstalk between macrophage metabolism and peritoneal tumors. J Clin Invest. 2018;128:3794–805.

52. Michelucci A, Cordes T, Ghelfi J, Pailot A, Reiling N, Goldmann O, Binz T, Wegner A, Tallam A, Rausell A, et al. Immune-responsive gene 1 protein links metabolism to immunity by catalyzing itaconic acid production. Proc Natl Acad Sci U S A. 2013;110:7820–5.

Figures

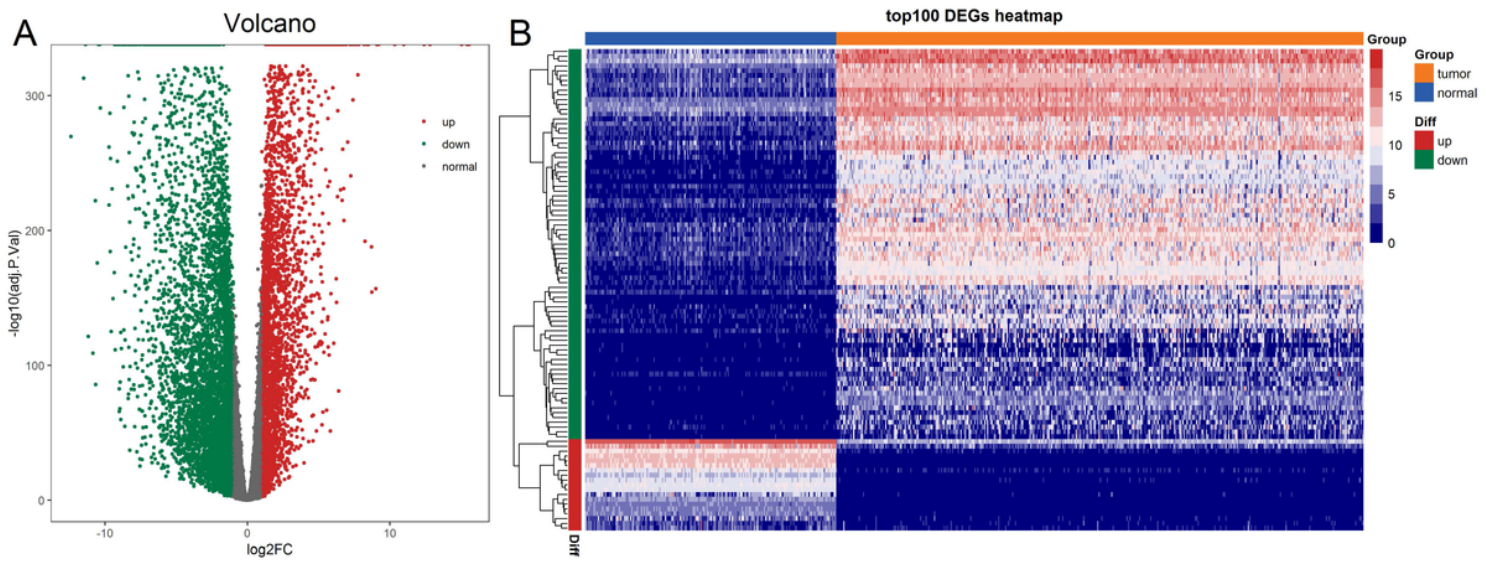

Figure 1

Distribution of DEGs. (A) Volcano map of DEGs. Red represents up-regulated genes, green represents down-regulated genes, and gray represents genes without significant differential expression. (B) Cluster heatmap of the top 100 DEGs. DEGs, differentially expressed genes.

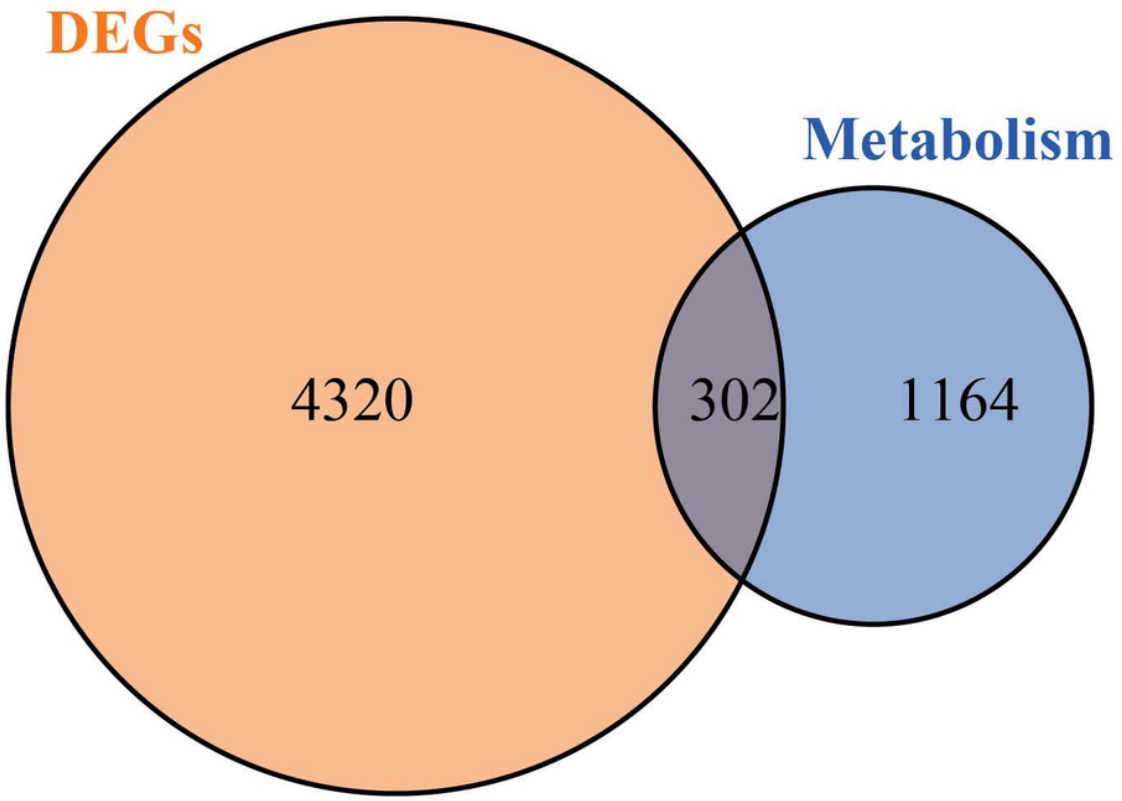

Figure 2

Venn diagram of metabolism-related DEGs. Orange indicates DEGs between normal and tumor tissues, blue indicates metabolic genes identified in KEGG pathways, and the overlapping section indicates metabolism-related DEGs. DEGs, differentially expressed genes.

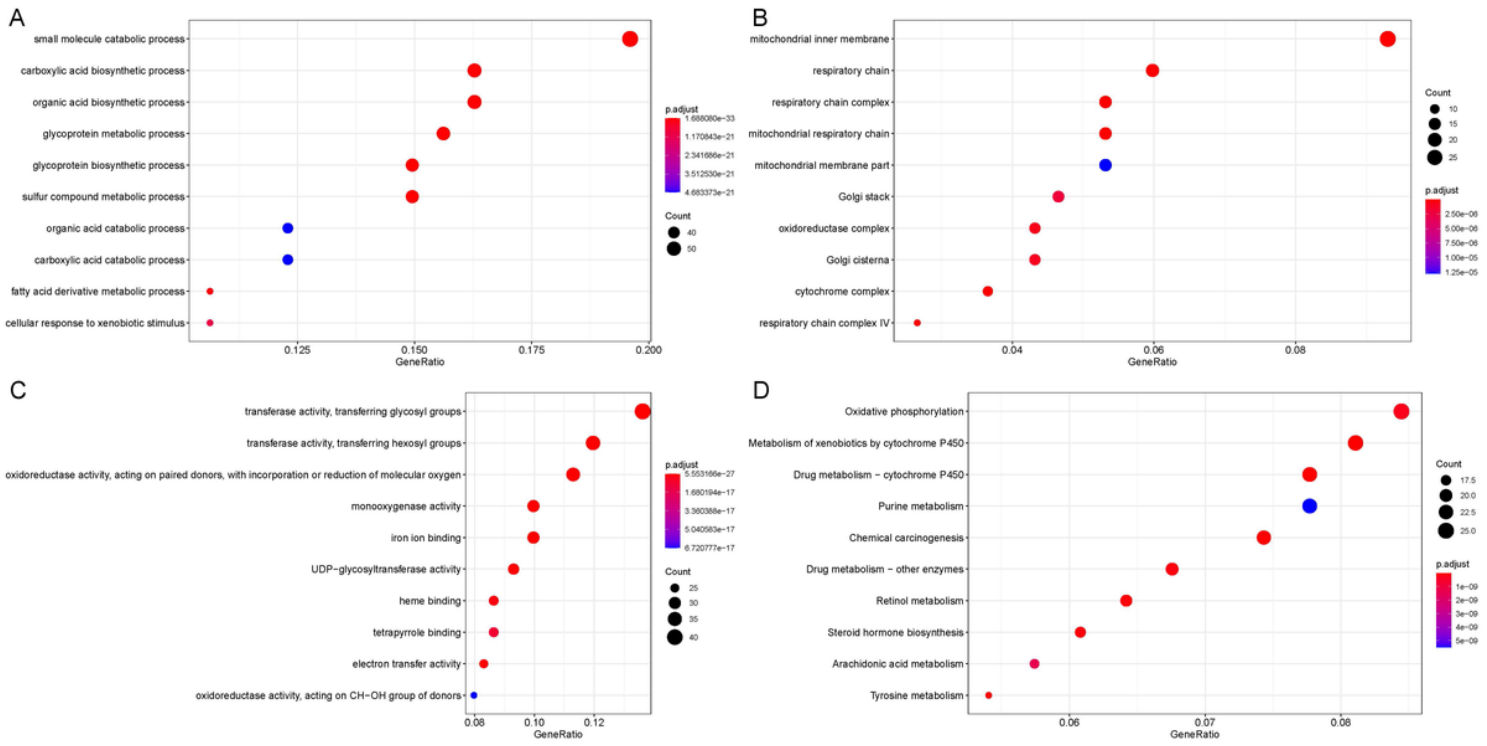

Figure 3

Functional enrichment analysis of 302 metabolism-related DEGs. (A) Results of GO-BP enrichment analysis. (B) Results of GO-CC enrichment analysis. (C) Results of GO- MF enrichment analysis. (D) Results of KEGG enrichment analysis. DEGs, differentially expressed genes. GO, Gene Ontology. BP, Biological Processes. MF, Molecular Functions. CC, Cellular Components. KEGG, Kyoto Encyclopedia of Genes and Genomes.

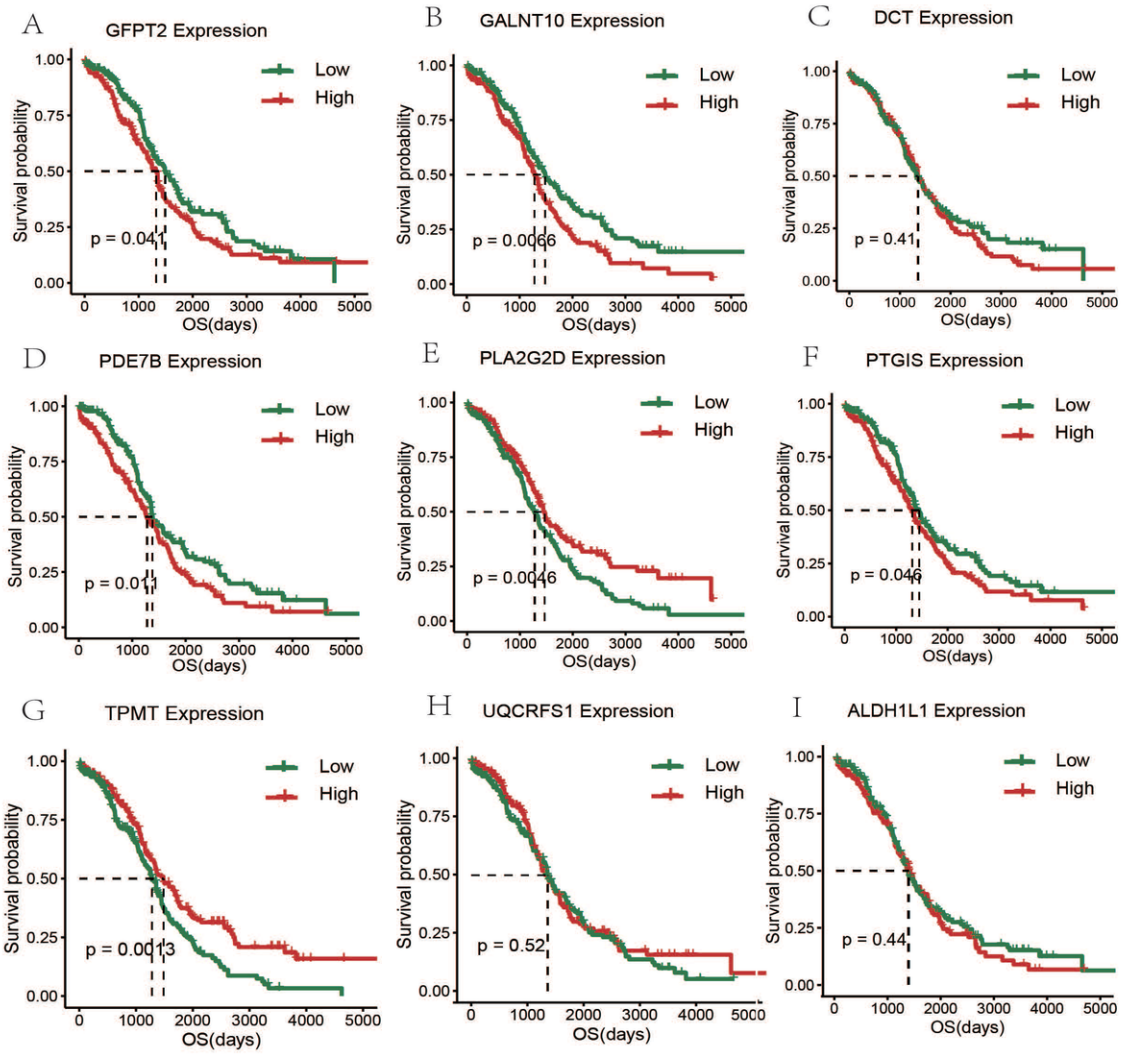

Figure 4

Kaplan-Meier survival analysis. A-I. Green represents low-risk group and red represents high-risk group. Single-factor Cox regression of the first 9 gene, samples were divided into high- and low-risk groups according to gene expression values, and the differences between the two groups were tested by log-rank.

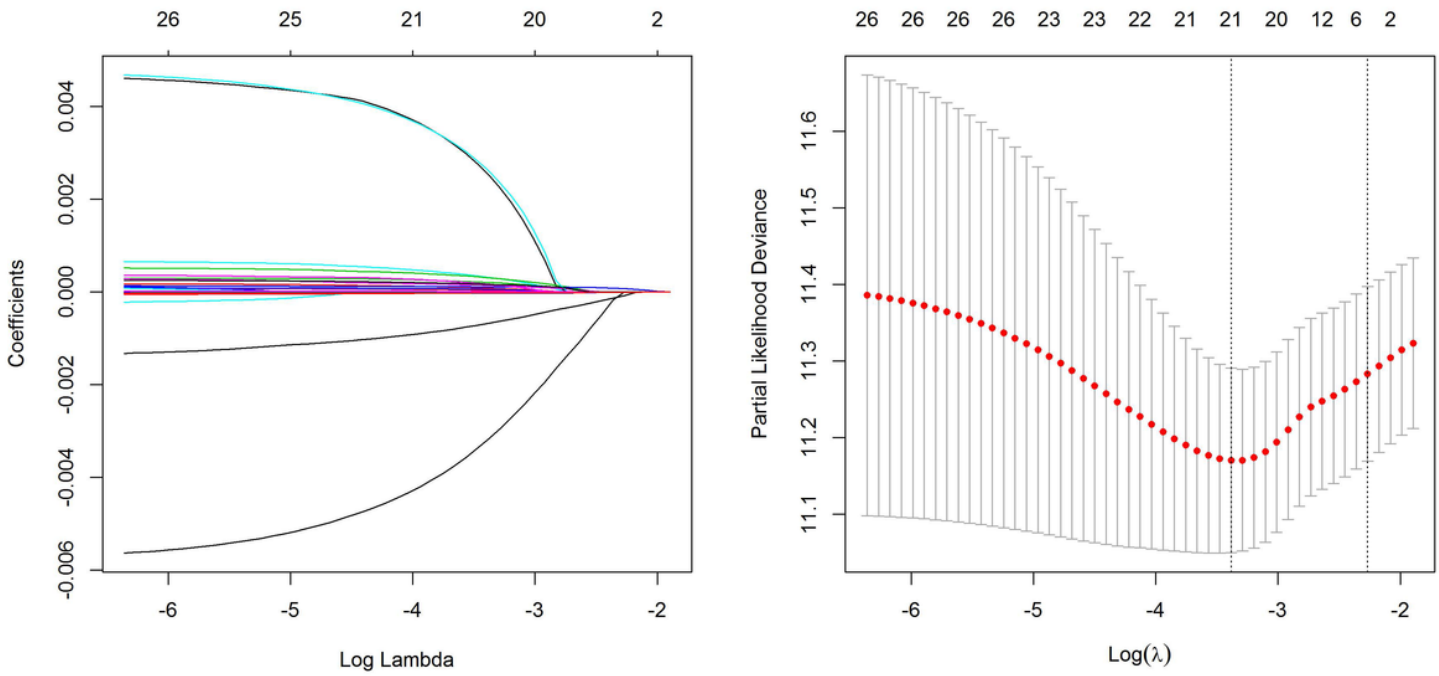

Figure 5

Construction of the prognostic model for OC. (A) LASSO coefficients of metabolism-related genes. Each curve represents a metabolic gene. (B) 1000-fold cross-validation for variable selection in the LASSO regression via min criteria.

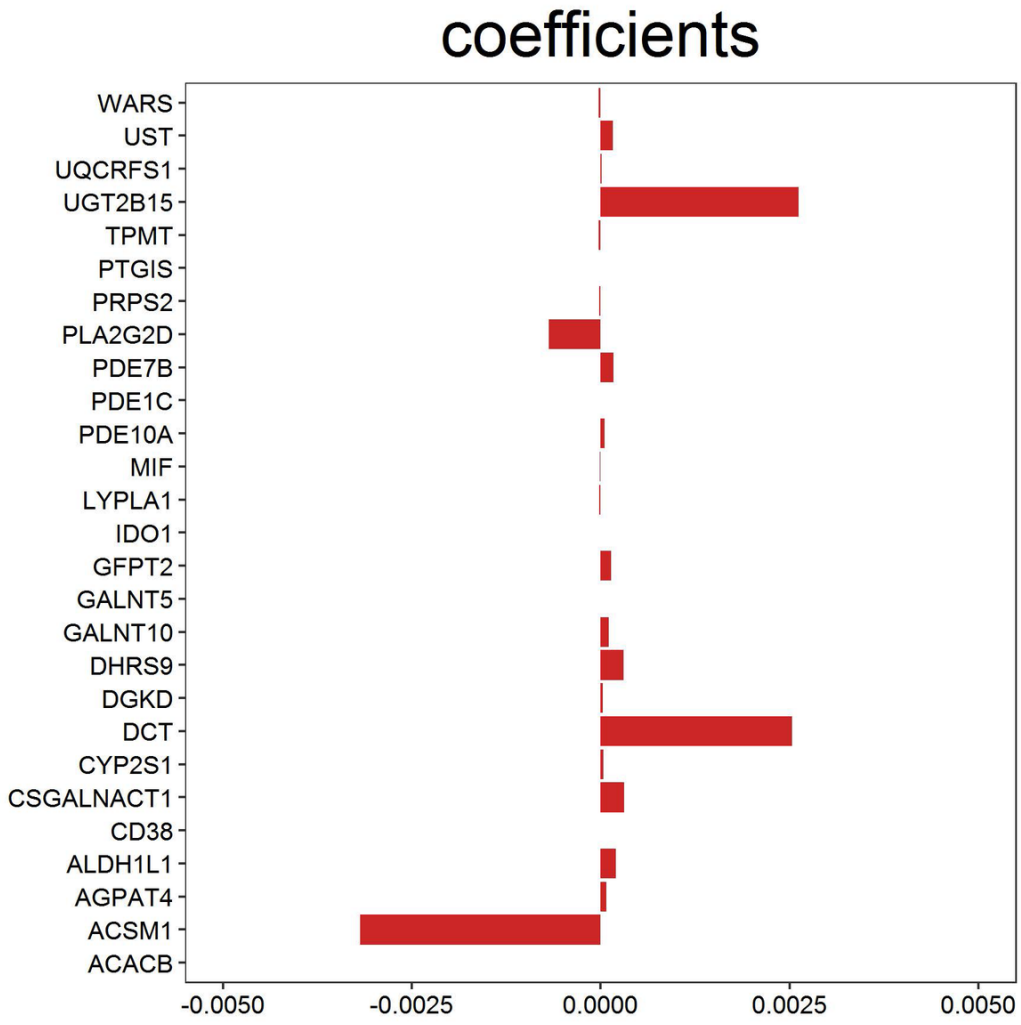

Figure 6

Two-sided standardized graph of LASSO regression results.

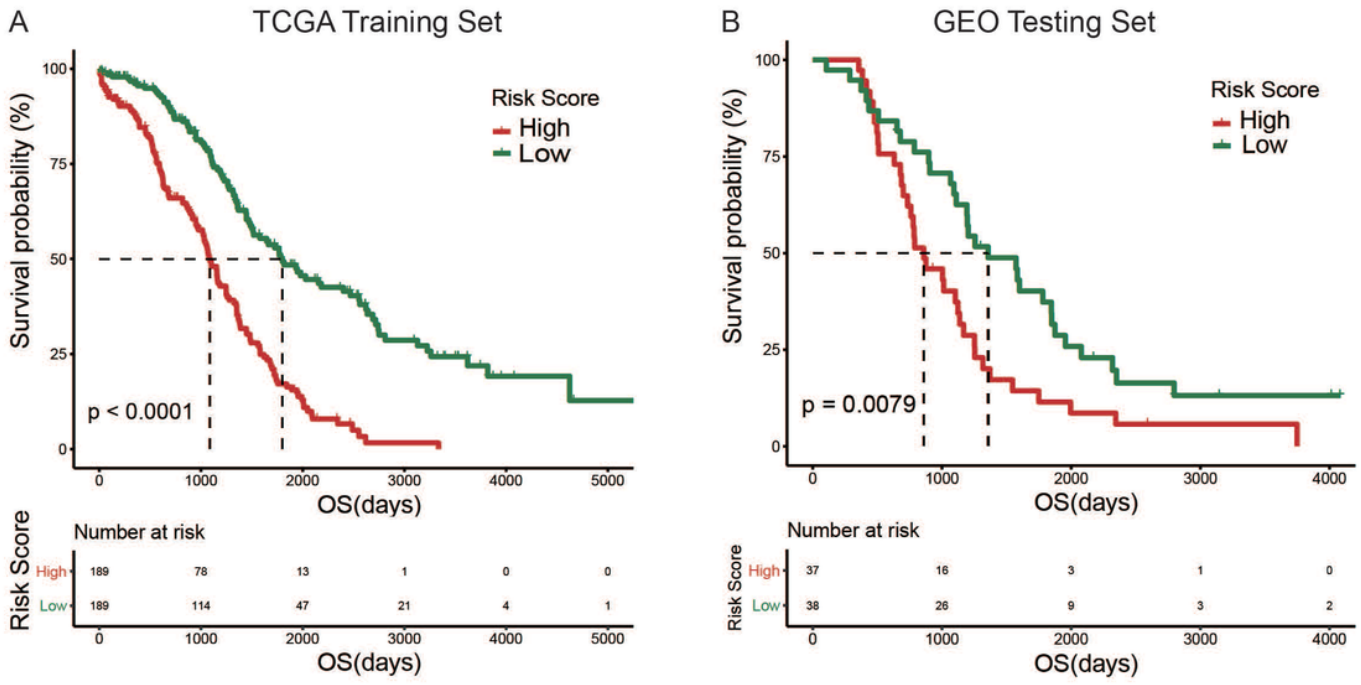

Figure 7

Construction and validation of the prognostic signature of the metabolism-associated gene. (A) Training set Kaplan-Meier survival analysis. (B) Validation set Kaplan-Meier survival analysis. High- and low-risk groups based on risk scores, green indicates low-risk group and red indicates high-risk group.

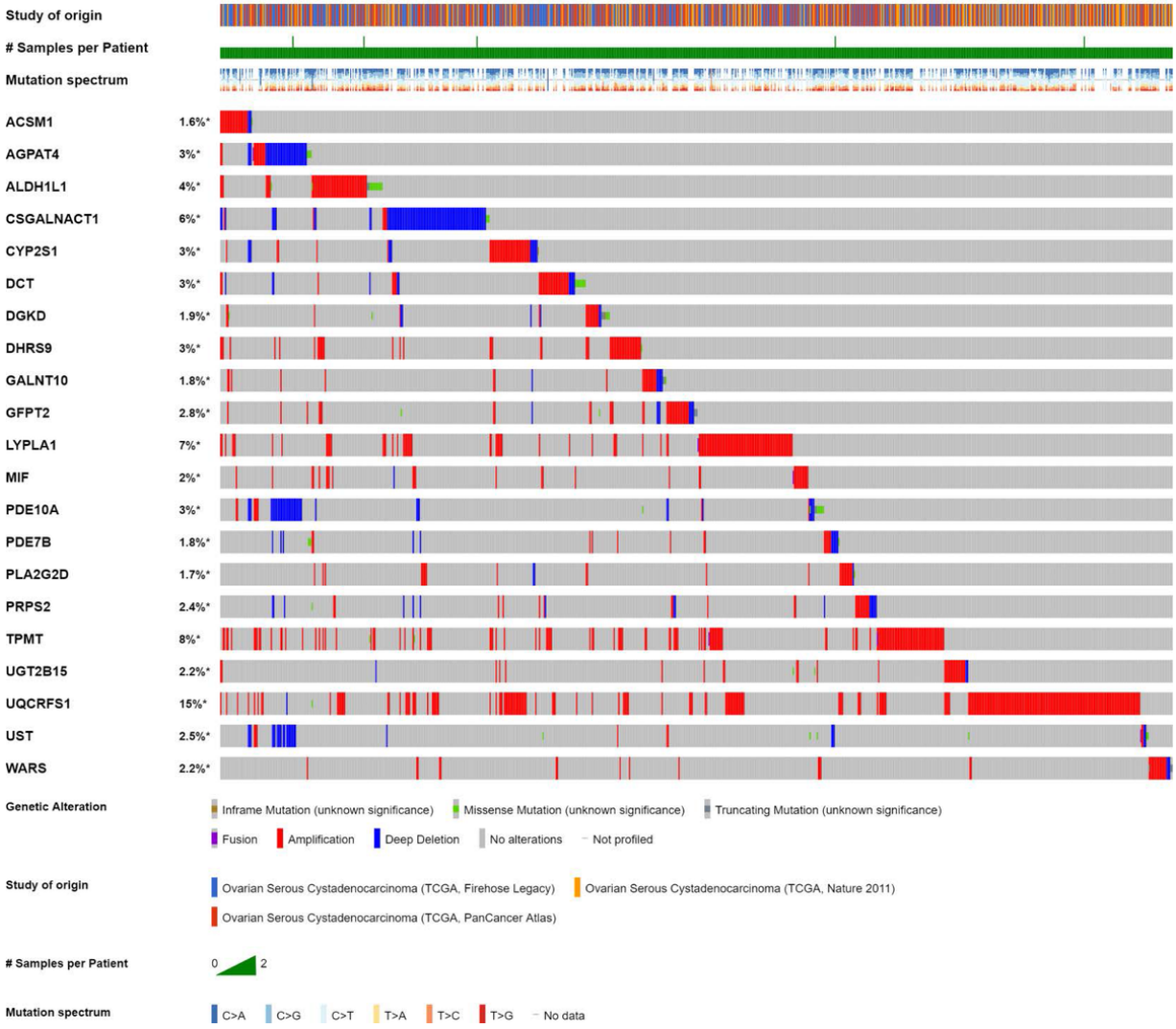

Figure 8

Genetic alteration of the prognostic genes in the gene signature (cBioportal).

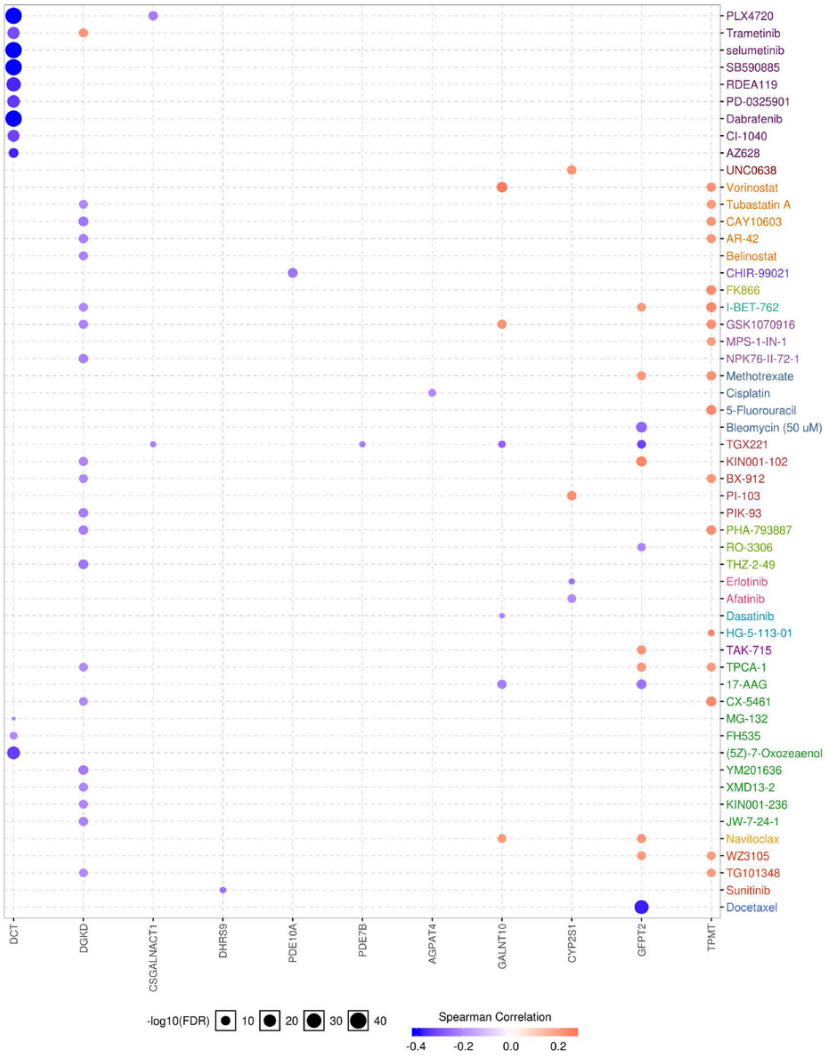

Figure 9

Drug sensitivity analysis of the prognostic genes in the gene signature (GSCALite). The expression of the prognostic genes in the gene signature was performed by Spearman correlation analysis with drug sensitivity. The positive correlation implies that high expression of the prognostic genes in the gene signature is resistant to the drug, and vice versa.

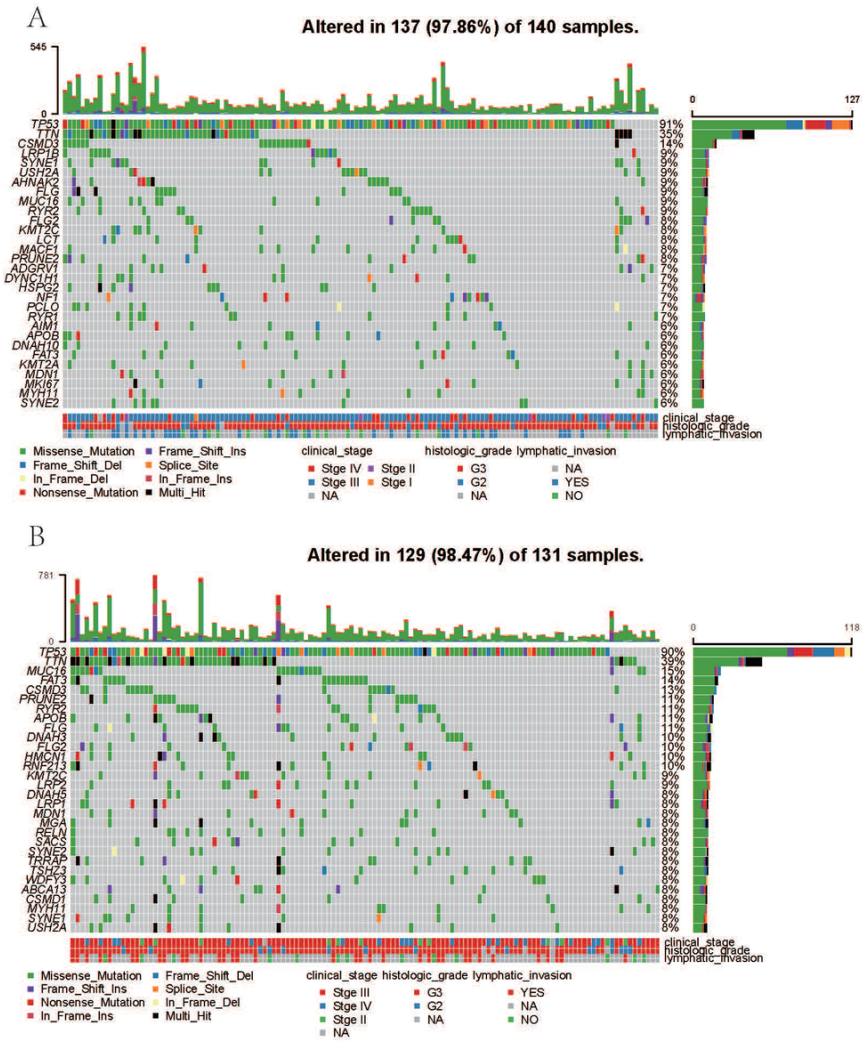

Figure 10

High- and low-risk groups mutation spectrums. (A) Gene mutation spectrum of the high-risk group. (B) Mutation spectrum of the low-risk group.

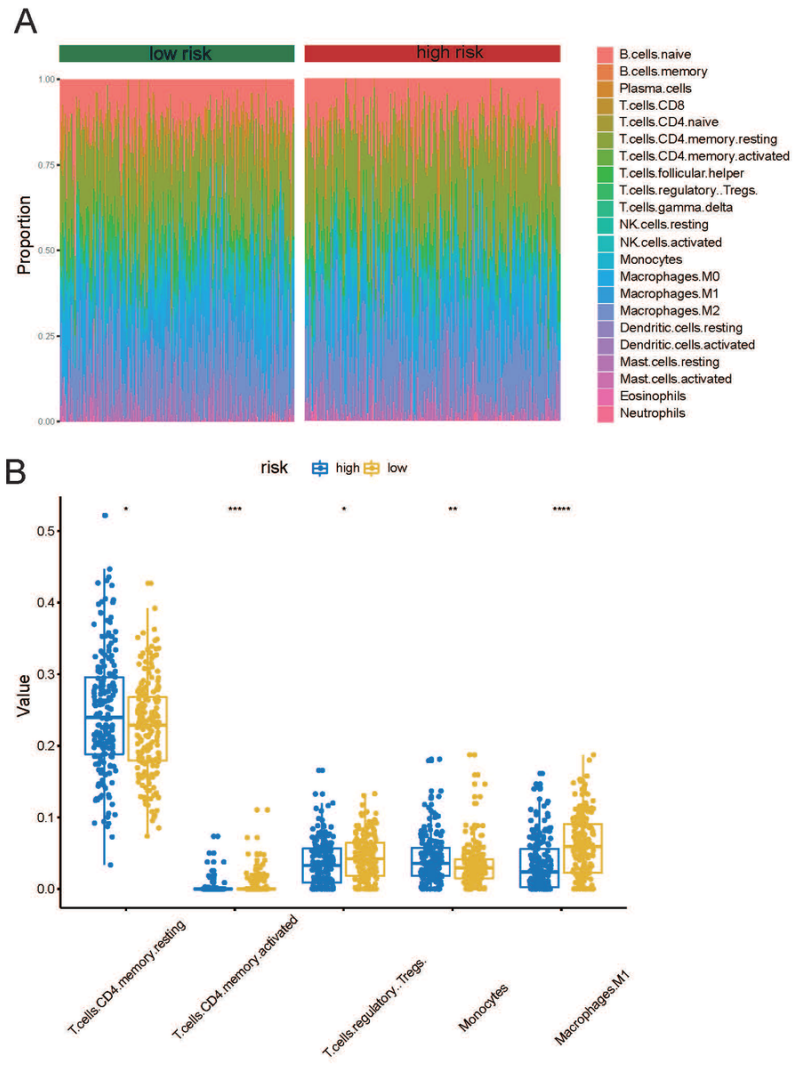

Figure 11

Differences in immune cell infiltration between high- and low-risk groups. (A) Proportion of 22 immune cells infiltrated in high- and low-risk samples. (B) Five immune cell types that showed significant differences between high- and low-risk groups and their expression between high- and low-risk groups.

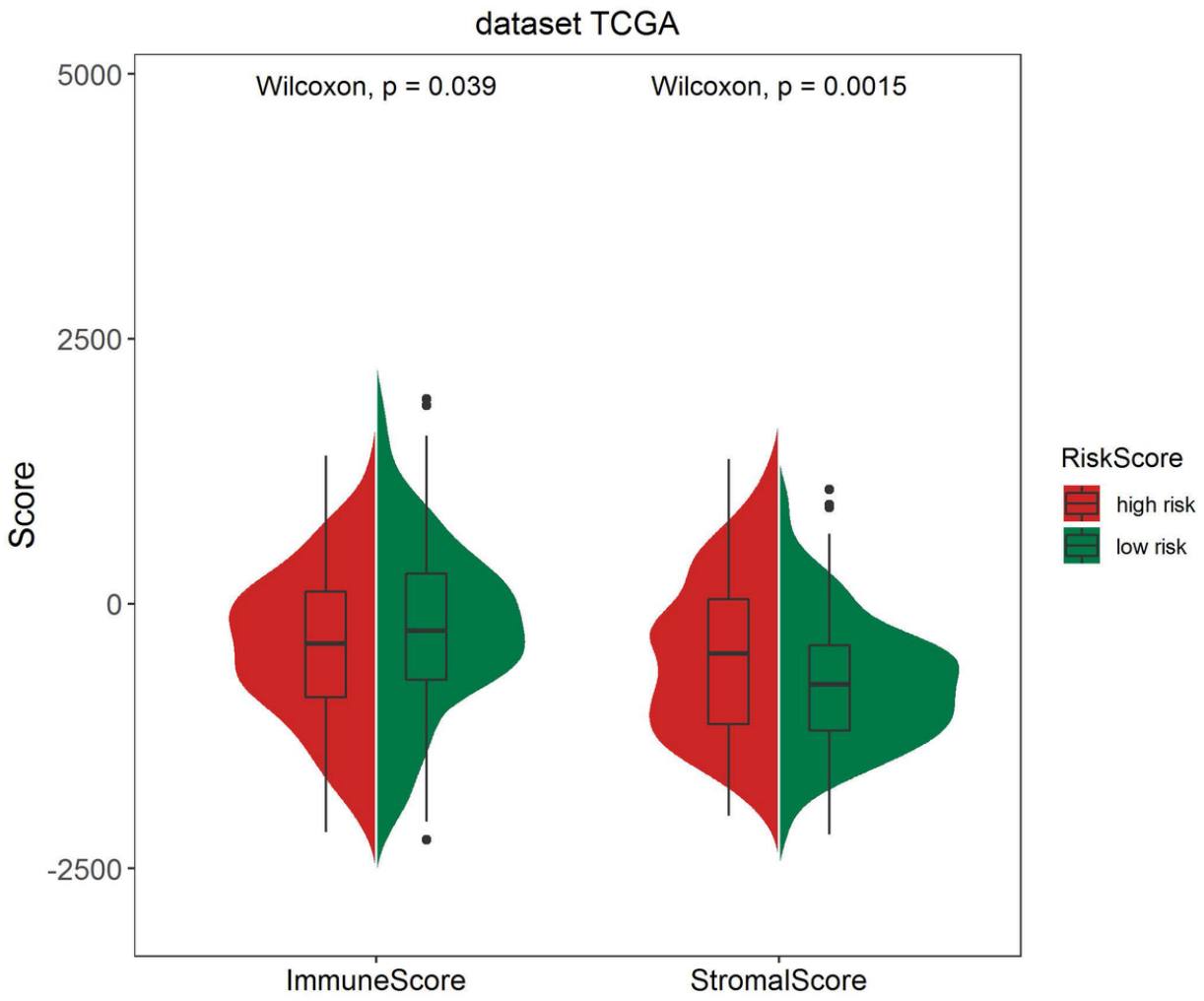

Figure 12

Immune score and matrix score in the high- and low-risk groups. Red represents the high-risk group and green represents the low-risk group.